The 4th International Conference on Vulnerability and Risk Analysis and Management (ICVRAM 2024)
the 8th International Symposium on Uncertainty Modelling and Analysis (ISUMA 2024)
April 25-28, 2024, Shanghai, China

First Excursion Probability Sensitivity by means of Multidomain Line Sampling

Mauricio A. Misraji[a], Marcos A. Valdebenito[a], Danko J. Jerez[b], Héctor A. Jensen[b], Michael Beer[c,d,e], and Matthias G.R. Faes[a]

[a]*Chair for Reliability Engineering, TU Dortmund University, Dortmund 44227, Germany, E-mail: {mauricio.misraji,marcos.valdebenito,matthias.faes}@tu-dortmund.de.*
[b]*Departamento de Obras Civiles, Universidad Técnica Federico Santa María, Valparaíso 2390123, Chile, E-mail: {danko.jerez,hector.jensen}@usm.cl.*
[c]*Institute for Risk and Reliability, Leibniz University Hannover, Hannover 30167, Germany, E-mail: beer@irz.uni-hannover.de.*
[d]*Institute for Risk and Uncertainty, University of Liverpool, Peach Street, Liverpool, L69 7ZF, United Kingdom*
[e]*International Joint Research Center for Engineering Reliability and Stochastic Mechanics, Tongji University, 1239 Siping Road, Shanghai, 200092, China*

Abstract

This contribution proposes a novel approach to estimate the first excursion probability and its sensitivity, leveraging the multidomain Line Sampling methodology to assess the reliability sensitivity of large-scale finite element models. The work is focused on linear structural systems subjected to a Gaussian loading, where the sensitivity is calculated with respect to deterministic structural parameters. The results indicate that the proposed framework excels in certain cases in terms of both accuracy and efficiency when compared to a similar method.

Keywords: first excursion probability; sensitivity analysis; Gaussian loading; linear structure; multidomain Line Sampling.

1. Introduction

In the context of structural dynamics, the safety level can be quantified by means of the so-called first excursion probability. This quantity measures the probability of one or more responses of interest exceeding a prescribed threshold as a result of a stochastic excitation [1]. The specific case where the behavior of the system remains linear and the stochastic loading is modelled as a Gaussian process brings important advantages, which have been addressed through several methods. Examples of the latter include a very efficient Importance Sampling (EIS) approach [2], the Domain Decomposition Method (DDM) [3], Directional Importance Sampling (DIS) [4] and lastly, multidomain Line Sampling (mLS) [5].

First excursion probabilities may, however, be highly sensitive to changes in structural properties, such as alterations in mass, stiffness, or geometrical dimensions of structural members. Therefore, quantifying the influence of these parameters on the first excursion probability becomes paramount for reliability assessment purposes [6]. Such information can be very useful in the context of risk evaluation, decision making, as well as reliability-based design optimization problems [7]. A possible means to quantify this sensitivity is calculating the gradient of the failure probability with respect to structural properties. The estimation of the gradient of the failure probability is a challenging task that has been explored in the literature in the past, see e.g. [8] and [9]. Within this research branch, the gradient of the failure probability can be calculated with respect to two different types of parameters [10]. First, it can be calculated with respect to distribution parameters of random variables, which are linked with the description of uncertain structural properties [11]. Second, it can be calculated with respect to deterministic structural behavior-related parameters [6,12], which is the focus of this work.

This paper introduces a framework for estimating the first excursion probability and its sensitivity based on multidomain Line Sampling, with emphasis on assessing the reliability sensitivity of large-scale finite element models. The investigation concentrates on linear structural systems subjected to a Gaussian loading, where sensitivity is calculated with respect to changes in deterministic structural parameters. In this regard, the use of multidomain Line Sampling plays a key role to obtain a precise estimator of sensitivity. That stems from the way the sampling method approaches the limit state hypersurface, demonstrating a notable enhancement when contrasted with a comparable method [13]. Furthermore, the sensitivity estimator is achieved as a byproduct of the reliability analysis [14] together with a sensitivity analysis of the spectral properties of the system [15]. For illustration purposes, the scheme is applied to a large-scale finite element model.

2. Problem Statement

2.1. Gaussian Loading

Assume that the dynamic loading acting on a given structural system is modeled as a discrete Gaussian process of duration T, discretized in n_T time instants of duration Δt, where the k-th time instant is defined as $t_k = (k-1)\Delta t, k = 1, \dots, n_T$. The loading is represented as a Karhunen-Loève expansion (see e.g. [16] and [17]) and is expressed as:

$$p(t_k, \boldsymbol{z}) = \mu_k + \boldsymbol{\psi}_k^T \boldsymbol{z}, \tag{1}$$

where p represents the load at time t_k; $\boldsymbol{z}$ is a realization of a standard Gaussian random variable vector $\boldsymbol{Z}$ of dimensions $n_{KL} \times 1$, being n_{KL} the order of truncation of the expansion ($n_{KL} \leq n_T$); μ_k is the mean value of the stochastic process at time t_k (assumed as zero); and $\boldsymbol{\psi}_k$ is a $n_{KL} \times 1$ vector containing the information on the covariance of the Gaussian process.

2.2. Structural System

The equation of motion associated with a linear elastic and classically damped structural system [19] is given by:

$$\begin{aligned} \boldsymbol{M}(\boldsymbol{y})\ddot{\boldsymbol{x}}(t, \boldsymbol{y}, \boldsymbol{z}) + \boldsymbol{C}(\boldsymbol{y})\dot{\boldsymbol{x}}(t, \boldsymbol{y}, \boldsymbol{z}) + \boldsymbol{K}(\boldsymbol{y})(t, \boldsymbol{y}, \boldsymbol{z}) \\ = \boldsymbol{g}(\boldsymbol{y})p(t, \boldsymbol{z}), t \in [0, T], \end{aligned} \tag{2}$$

where $\boldsymbol{x}$, $\dot{\boldsymbol{x}}$ and $\ddot{\boldsymbol{x}}$ are vectors representing the displacement, velocity and acceleration, respectively, all with dimensions $n_D \times 1$; the matrices of mass $\boldsymbol{M}$, damping $\boldsymbol{C}$ and stiffness $\boldsymbol{K}$, are of dimension $n_D \times n_D$; the coupling vector of the loading with the degrees-of-freedom is $\boldsymbol{g}$, which has dimensions $n_D \times 1$; and the vector $\boldsymbol{y}$ of dimension $n_Y \times 1$ comprises the parameters representing the structural properties of the system, which may be subject to potential changes influenced by practical design decisions [18]. For example, parameters contained in $\boldsymbol{y}$ could be related to the geometry of structural members (such as cross section or length), or material properties (such as Young's Modulus), among others.

Effectively managing certain dynamic responses, like displacements, accelerations, and internal stresses, is of utmost importance. These responses of interest are defined as $\eta_i(t, \boldsymbol{y}, \boldsymbol{z}), i = 1, \dots, n_\eta$, and are calculated using the convolution integral [19]:

$$\begin{aligned} \eta_i(t, \boldsymbol{y}, \boldsymbol{z}) = \int_0^t h_i(t-\tau, \boldsymbol{y}) p(\tau, \boldsymbol{z}) d\tau, \\ i = 1, \dots, \eta_\eta, \end{aligned} \tag{3}$$

where h_i is the unit impulse of the i-th interest response function, which can me calculated by modal analysis [19]. Equation (3) is deduced under the assumption of null initial conditions.

Considering the time discretization defined in Section 2.1, the responses of interest are given by:

$$\eta_i(t_k, \boldsymbol{y}, \boldsymbol{z}) = \boldsymbol{a}_{i,k}(\boldsymbol{y})^T \boldsymbol{z}, \tag{4}$$

where $\boldsymbol{a}_{i,k}(\boldsymbol{y})$ is a vector of dimension $n_{KL} \times 1$ which is defined as:

$$\boldsymbol{a}_{i,k}(\boldsymbol{y}) = \sum_{m=1}^{k} \Delta t \epsilon_m h_i(t_k - t_m, \boldsymbol{y}) \boldsymbol{\psi}_m, \tag{5}$$

where ϵ_m is chosen according to the adopted integration rule [20]. For example, using the trapezoidal rule $\epsilon_m = 1/2$ if $m = 1$ or $m = k$; otherwise $\epsilon_m = 1$.

2.3. First Excursion Probability

The design criteria vector $\boldsymbol{b}$ has dimensions $n_\eta \times 1$, where b_i is its i-th element and correspond to the prescribed threshold for the η_i response of interest. Therefore, the performance function $g(\boldsymbol{y}, \boldsymbol{z})$ indicates whether the response of interest η_i exceeds a prescribed threshold b_i within the duration of the stochastic loading, and is given by:

$$\begin{aligned} & g(\boldsymbol{y}, \boldsymbol{z}) \\ & = 1 - \max_{i=1,\dots,n_\eta} \left(\max_{k=1,\dots,n_T} \left(\frac{|\eta_i(t_k, \boldsymbol{y}, \boldsymbol{z})|}{b_i} \right) \right), \end{aligned} \tag{6}$$

where $|\cdot|$ denotes absolute value. It is worth noting that the event in which a single response of interest η_i exceeds the prescribed threshold b_i at a specific time instant t_k defines the elementary failure event $F_{i,k}$. Furthermore, the failure domain can be formally defined as $F = \{\boldsymbol{z} \in \mathbb{R}^{n_{KL}} : g(\boldsymbol{y}, \boldsymbol{z}) \leq 0\}$, which corresponds to the union of all the elementary failure domains. The probability associated with the failure domain can be quantified by means of the so-called first excursion probability [1]:

$$p_F(\boldsymbol{y}) = \int_{g(\boldsymbol{y}, \boldsymbol{z}) \leq 0} f_{\boldsymbol{Z}}(\boldsymbol{z}) d\boldsymbol{z}, \tag{7}$$

being $f_{\boldsymbol{Z}}(\cdot)$ the standard Gaussian probability density function in n_{KL} dimensions. Equation (7) corresponds to an n_{KL}-dimensional integral which does not have a closed-form solution and cannot be calculated analytically. Indeed, Equation (6) comprises a composition of $n_\eta \times n_T$ linear elementary failure domains with significant degree of overlap between

them, as discussed in detail in [21]. Various simulation techniques have been developed to address this challenging problem, taking advantage of the system linearity; see, indicatively, [2,3,4].

2.4. *Sensitivity of First Excursion Probability*

The first excursion probability, as shown in Equation (7), has a clear dependency on the design parameters vector $\boldsymbol{y}$. Therefore, it is of paramount interest to determine the sensitivity of this failure probability with respect to the design parameters. One potential approach to measure that sensitivity is to calculate the gradient of the first excursion probability with respect to a design parameter y_j, which can be written as [23]:

$$\frac{\partial p_F(\boldsymbol{y})}{\partial y_j} = -\int_{g(\boldsymbol{y},\boldsymbol{z})=0} \frac{\partial g(\boldsymbol{y},\boldsymbol{z})}{\partial y_j} \frac{1}{\|\nabla_{\boldsymbol{z}} g(\boldsymbol{y},\boldsymbol{z})\|} f_{\boldsymbol{Z}}(\boldsymbol{z}) dS, \quad (8)$$

where $p_F(\boldsymbol{y})$ denotes the first excursion probability, $g(\boldsymbol{y},\boldsymbol{z})$ is the performance function, and $\boldsymbol{z}$ represents a realization of a standard Gaussian random variable $\boldsymbol{Z}$. Additionally, $\|\cdot\|$ denotes the Euclidean norm; ∇_z is the Nabla operator; $f_{\boldsymbol{Z}}(\boldsymbol{z})$ is the standard Gaussian probability density function; and dS denotes a differential element of the limit state hypersurface, that is $g(\boldsymbol{y},\boldsymbol{z}) = 0$. Although Equation (8) does not have an analytical solution for most cases, different advanced simulation methods can be used to calculate it.

3. Multidomain Line Sampling

3.1. *First Excursion Probability by means of mLS*

The elementary failure domains described in Section 2.4, as shown in [21], correspond to a series of hyperplanes, where each failure domain $F_{i,k}$ can be decomposed into the positive part of the domain $F_{i,k}^{+}$, and in the negative part of the domain $F_{i,k}^{-}$. Any of them takes place if the response of interest exceeds the prescribed threshold in the positive direction, where $\eta_{i,k} \geq b_i$; or in the negative direction, where $\eta_{i,k} \leq -b_i$. In each case, the resulting hypervolume associated with the failure region is bounded by a hyperplane, which is a consequence of the system linearity. For further clarification of the aforementioned idea, Figure 1 illustrates a two-dimensional representation of the failure domain geometry for the case where $n_\eta = 1$ and $n_T = n_{KL} = 2$. Here, $F_{1,1}$ and $F_{1,2}$ are elementary failure domains which are decomposed in their positive and negative symmetric subdomains. In this example, it is straightforward to note that the failure domain is $F = F_{1,1} \cup F_{1,2}$, and the overlap between the elementary failure domains is represented by the dark red color in the interacting regions.

The estimation of the failure probability, leveraging the linearity of the system, has been addressed by several methods in the literature [2,3,4], and lastly by multidomain Line Sampling [5]. It has been demonstrated that the failure probability p_F showed in Equation (7) can be written as:

$$p_F(\boldsymbol{y}) = \sum_{i=1}^{n_\eta} \sum_{k=1}^{n_T} p_{i,k}(\boldsymbol{y}), \quad (9)$$

where $p_{i,k}$ denotes the *effective* contribution to the failure probability of the failure event $F_{i,k}$, which can be calculated as it follows:

$$p_{i,k}(\boldsymbol{y}) = \int_{\boldsymbol{z}\in F_{i,k}} \frac{1}{\sum_{l=1}^{n_\eta}\sum_{m=1}^{n_T} I_{F_{l,m}}} f_{\boldsymbol{Z}}(\boldsymbol{z}) d\boldsymbol{z}, \quad (10)$$

where $I_{F_{i,k}}(\boldsymbol{y},\boldsymbol{z})$ is an indicator function which is equal to 1 if $\boldsymbol{z} \in F_{i,k}$ and 0 in other case.

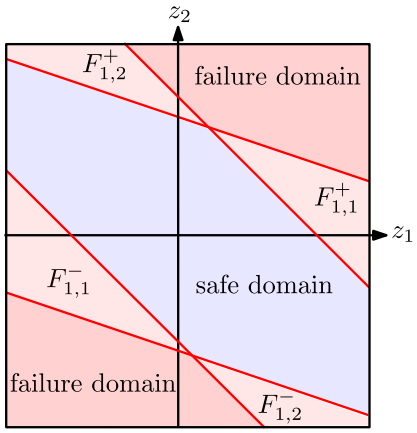

Figure 1: Two-dimensional representation of the failure domain geometry.

The effective contributions can be efficiently calculated by means of Line Sampling [22]. The estimation of $p_{1,1}$ is illustrated schematically in Figure 2 following the same two-dimensional case showed before. It can be seen that $\boldsymbol{\alpha_1}$ represents the so-called important direction and is pointing towards $F_{1,1}^{+}$, which can be calculated based on the discretized response of interest shown in Equation (4). From this vector, the coordinates $z_1^{\parallel}$ and $\boldsymbol{z}_1^{\perp}$ can be defined, where $z_1^{\parallel}$ points in the direction parallel to the important direction $\boldsymbol{\alpha}_1$, and $\boldsymbol{z}_1^{\perp}$ points in the orthogonal direction to the important direction $\boldsymbol{\alpha}_1$. The way Line Sampling estimates the effective contribution $p_{1,1}$ is through simulation. It generates a random sample from to the coordinate set $\boldsymbol{z}_1^{\perp}$ (denoted as $\boldsymbol{z}_1$ in Figure 2), and then

calculates the integral along the green line (parallel to $\boldsymbol{\alpha}_1$). It is important to note that the integral calculation is performed over the elementary failure domain $F_{1,1}$, represented by the solid part of the green line. Moreover, the calculation of the responses of interest along a line involves two dynamic analyses, one associated with the parallel component and one with the perpendicular component [5].

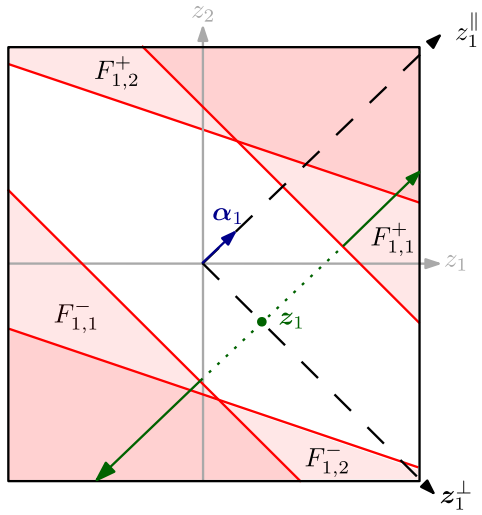

Figure 2: Application of Line Sampling for estimating the effective contribution $p_{1,1}$

In practical implementation of multidomain Line Sampling, instead of explicitly calculating all effective contributions $p_{i,k}$ as outlined in Equation (9), the summation is estimated via simulation [3] by incorporating the weights $\omega_{i,k}$. A very convenient choice of the weights is to be proportional to the probability of occurrence of the event $F_{i,k}$, as depicted in [2]. The weights can be calculated as:

$$\omega_{i,k} = \frac{P[F_{i,k}]}{\sum_{l=1}^{n_\eta}\sum_{m=1}^{n_T} P[F_{l,m}]}, \tag{11}$$

where $P[F_{i,k}]$ is the probability of failure associated with the elementary failure event $F_{i,k}$. It can be noted that the denominator corresponds to an upper bound for the failure probability [2]. Therefore, Equation (9) can be written as follows:

$$p_F(\boldsymbol{y}) = \sum_{i=1}^{n_\eta}\sum_{k=1}^{n_T}\left(\frac{p_{i,k}(\boldsymbol{y})}{\omega_{i,k}}\right)\omega_{i,k}\,. \tag{12}$$

The incorporation of the weights $\omega_{i,k}$ can be interpreted as the probability mass function of a discrete random variable. Therefore, combining the last definitions it is possible to calculate the failure probability by means of simulation as:

$$p_F(\boldsymbol{y}) \approx \tilde{p}_F(\boldsymbol{y}) = \frac{1}{N}\sum_{j=1}^{N}\left(\frac{1}{\omega_{i,k}^{\{j\}}}p_{i,k}^{\{j\}}\left(\boldsymbol{y}, \boldsymbol{z}^{\perp,\{j\}}\right)\right), \tag{13}$$

where the pair(i,k) associated with the sample $\{j\}$ is randomly selected with probability proportional to the weights, and N is the total number of samples.

3.2. *Sensitivity of First Excursion Probability by means of mLS*

The sensitivity of the first excursion probability is directly related to the sensitivity of the limit state hypersurface associated with the failure domain. To exemplify how changes in the vector $\boldsymbol{y}$ affects its geometry, a two-dimensional case is considered, where the failure domain is constructed by the union of two elementary failure domains, with a single design parameter involved. In the Figure 3, $g(y_j, \boldsymbol{z}) < 0$ represents the failure domain, and $g(y_j, \boldsymbol{z}) > 0$ the safe domain, where the limit state function (red line) is perturbed (blue line) due to a change Δy_j in the design parameter y_j. The sensitivity estimator represents the quantification of the potential change in the failure probability resulting from this perturbation.

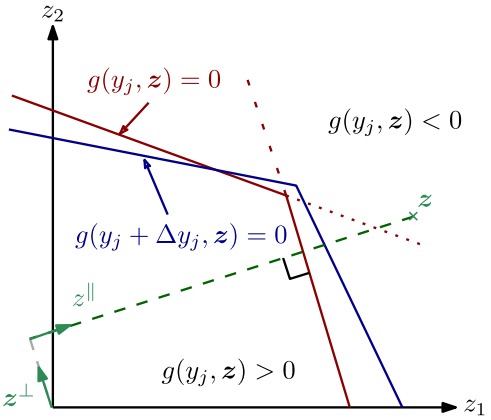

Figure 3: Two-dimensional representation of the sensitivity of the limit state function

In the case of multidomain Line Sampling, the dashed lines in Figure 3 illustrate how the exploration is performed. For a realization $\boldsymbol{z}$ of $\boldsymbol{Z}$, the failure domain is explored along a line that is perpendicular to one of the independent limit state functions, as is showcased in Section 3.1. Moreover, this change has an evident impact on the calculation of the effective contribution $p_{i,k}$, and consequently, in the first excursion probability estimator.

The sought sensitivity can be calculated taking the derivative of Equation (12) with respect to a design parameter $\mathrm{y_j}, \mathrm{j} = 1, \ldots, \mathrm{n_Y}$, resulting in:

$$\frac{\partial p_F(\boldsymbol{y})}{\partial y_j} = \sum_{i=1}^{n_\eta} \sum_{k=1}^{n_T} \left(\frac{1}{\omega_{i,k}} \frac{\partial p_{i,k}(\boldsymbol{y})}{\partial y_j} \right) \omega_{i,k}, \quad (14)$$

where the term $\partial p_{i,k}(\boldsymbol{y})/\partial y_j$ can be calculated using Leibniz' rule [23], primarily involving the derivative of the responses of interest. In turn, the convolution integral is involved, as shown in Equation (3) and its discretized form, as shown in Equation (4), which implies calculating the derivatives of the impulse response functions. These derivatives entail differentiating the spectral properties of the system (natural frequencies and mode shapes), a task widely explored in literature [24]. One advantageous approach from the computational effort standpoint is proposed by [15], which involves solving systems of linear equations associated with the structural matrices and their derivatives.

Ultimately, Equation (14) can also be computed through simulation, and its formulation is as follows:

$$\frac{\partial p_F(\boldsymbol{y})}{\partial y_j} \approx \frac{\partial \tilde{p}_F(\boldsymbol{y})}{\partial y_j} = \frac{1}{N} \sum_{j=1}^{N} \left(\frac{1}{\omega_{i,k}^{\{j\}}} \frac{\partial p_{i,k}^{\{j\}}\left(\boldsymbol{y}, \boldsymbol{z}^{\perp,\{j\}}\right)}{\partial y_j} \right), \quad (15)$$

where the pair (i,k) associated with the sample $\{j\}$ is randomly selected with probability proportional to the weights, and N is the total number of samples. It is worth noting that the level of precision of the sensitivity estimator can be quantified in terms of its coefficient of variation (see, e.g. [25]).

4. Numerical Example

The numerical example corresponds to a 3-D finite element model of a curved bridge which comprises 10068 degrees-of-freedom. The model is based on an example presented in [4]. The superstructure is modeled as a monolithic box girder which is represented through shell and beam elements. Regarding its geometry, is curved in the plane x-y with a total length of 119 [m], composed of five spans of length 24 [m], 20 [m], 23 [m], 25 [m], 27 [m], respectively. The substructure is modeled by means of four columns with diameter 1.6 [m] and height 8 [m]. Each of the columns is supported by four piles of 35 [m] length and diameter 0.6 [m]. The interaction between the piles and soil is modeled by means of linear springs with translational stiffness in x and y direction. A sketch of the curved bridge model is shown in Figure 4, where the columns are denoted as $C_k, k \in [1,2,3,4]$. The stiffness of the above-mentioned springs varies linearly from $k_s = 112$ [MN/m] at the deepest point of the pile up to 0 [MN/m] at the ground level. All the superstructure and substructure elements are modeled with the same material properties, being reinforced concrete with Young's modulus $E = 2.09 \times 10^{10}$ [N/m²], Poisson ratio $\nu = 0.2$ and density $\rho = 2500$ [kg/m³]. The classical damping considered is equal to 3% for all mode shapes.

The excitation acting on the bridge is modeled as a discrete white noise process of spectral intensity $S = 5 \times 10^{-4}$ [m²/s³], with a duration of $T = 10$ [s], discretized in 1001 time instants of duration $\Delta t = 0.01$ [s]. It is applied with an angle of 45 degrees as is shown in Figure 2.b. In addition, the white noise passes through a Clough-Penzien filter [26] and is modulated by the following function $m(t)$:

$$m(t) = \begin{cases} \left(\frac{t}{5}\right)^2 & 0 \le t \le 5 \text{ [s]} \\ 1 & 5 \le t \le 6 \text{ [s]} \\ e^{-(t-6)^2} & t > 6 \text{ [s]} \end{cases}. \quad (16)$$

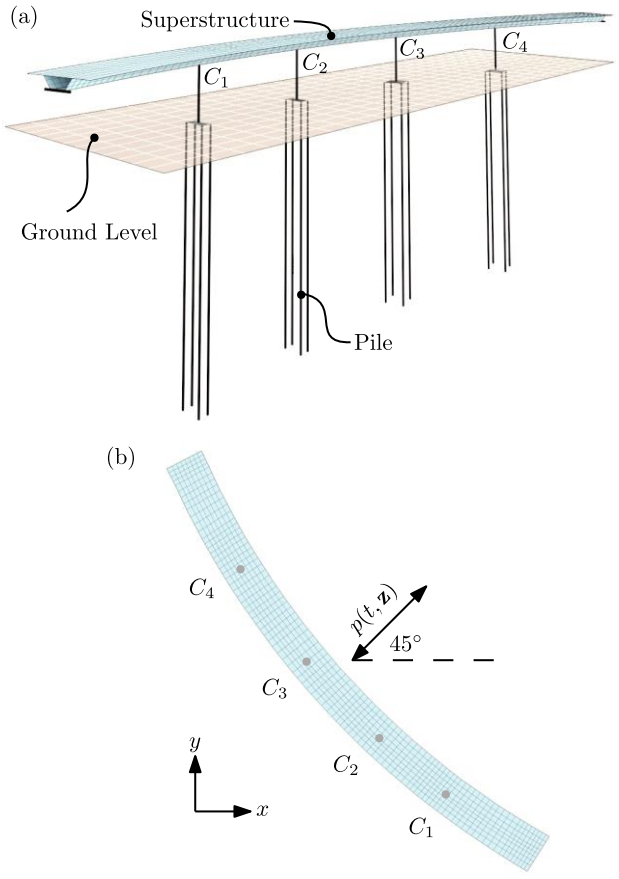

Figure 4: Curve bridge finite element model. (a) Perspective view; (b) Plan view

The assumption is made that the structure starts from a position of rest. The failure event is defined as

the drift of the columns (in either x or y direction) exceeding a threshold of $b = 0.02$ [m] within the duration of the stochastic excitation. It is a challenging problem which involves a large number of individual criteria (1001-time instants and 8 interest responses, a total of 8008 elementary failure domains). Moreover, for the dynamic analysis, a truncation to 100 mode shapes has been realized to ensure a correct representation of the response. The first excursion probability associated with this problem is calculated using mLS resulting in $\tilde{p}_F^{mLS} \approx 3.0 \times 10^{-3}$. The objective is, by using mLS, determining the sensitivity of the first excursion probability with respect to vector $\boldsymbol{y} = [y_1, \dots, y_4]^T$, where $y_j, j \in [1,2,3,4]$ denotes the diameter of the j-th column. The sensitivities calculation offers key information for assessing the bridge columns design to fulfill the serviceability requirements.

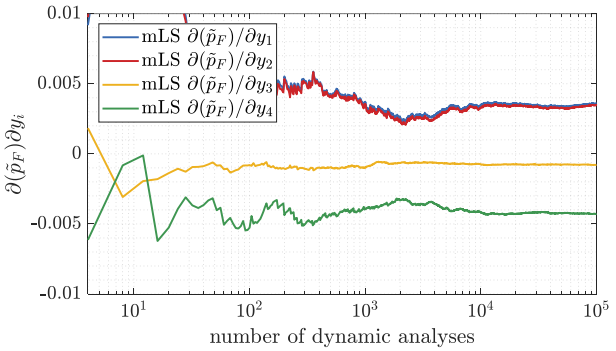

Figure 5: Estimators for the gradient of the first excursion probability

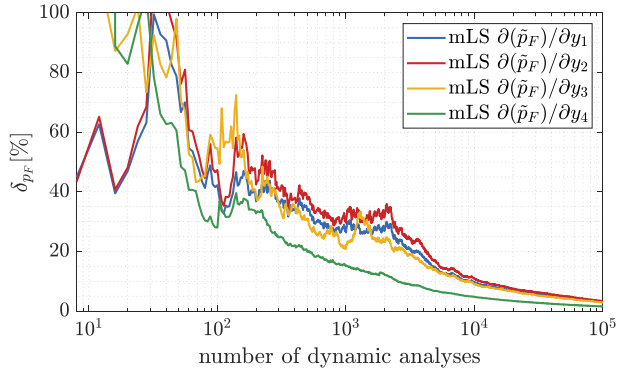

Figure 6: Coefficient of variation of the sensitivity estimators of the first excursion probability

The sensitivities of the first excursion probability with respect to the parameters y_j are calculated by both The evolution of the four estimates $\partial\tilde{p}_F(\boldsymbol{y})/\partial y_j$, and their associated coefficients of variation δ_{y_j}, with respect to the number of the performed dynamic analyses, are shown in Figure 5 and Figure 6. It can be observed that stable estimates can be achieved with a reduced number of dynamic analyses, reaching values close to a coefficient of variation of 20% with 4000 dynamic analyses in the worst case. After a large number of simulations, it is possible to identify the most recurrent failure mode, which involves a rotation of the bridge in a point between columns 1 and 2. In this regard, the results show that increasing the diameter of the columns C_3 and C_4, decreases the failure probability, which can be interpreted physically as opposing a potential rotation of the bridge (and reducing the drifts). On the other hand, increasing the diameter of columns C_1 and C_2, increases the failure probability, which can be interpreted as contributing a potential rotation of the bridge (and increasing the drifts).

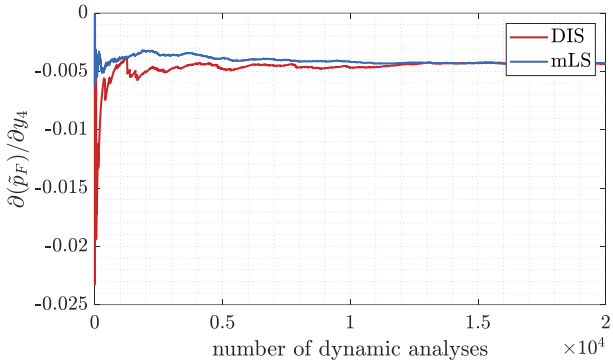

Figure 7: Sensitivity estimator with respect to design parameter y_4

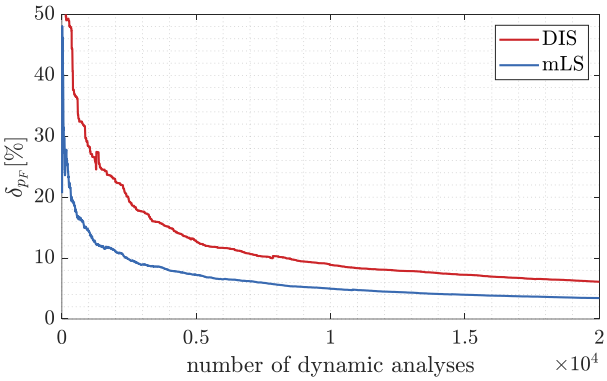

Figure 8: Coefficient of variation of sensitivity estimator with respect to design parameter y_4

Furthermore, in Figure 7 and Figure 8, a comparative analysis of the sensitivity estimator related to y_4 is depicted, showcasing the outcomes obtained through both mLS and Directional Importance Sampling (DIS) [13]. DIS serves as a comparable method, as it is also a simulation-based approach for gradient estimation. The comparison is presented in terms of the number of dynamic analyses needed to obtain a single value of the sensitivity estimator and its corresponding coefficient of variation. It is worth

noting that mLS requires two dynamic analyses and two sensitivity analyses for simulation, while DIS requires one dynamic analysis and one sensitivity analysis for simulation. Our findings reveal that the sensitivity estimator calculated using mLS requires fewer dynamic analyses to achieve a determined precision level when compared to the estimator calculated using DIS. Moreover, it is evident that mLS produces a more stable estimator than DIS, for the example under consideration.

5. Conclusions

This paper has examined the application of multidomain Line Sampling for estimating the sensitivity of the first excursion probability of a linear system subject to a Gaussian loading. The sensitivity of the first excursion probability is calculated as a byproduct of the reliability analysis. Additionally, the calculation involves the sensitivity analysis of the unit impulse response functions, as well as the spectral properties of the system.

The calculation of the sought sensitivities using multidomain Line Sampling is achieved with a reduced number of dynamic analyses, demonstrating improved efficiency and stability when compared with Directional Importance Sampling. One advantage of mLS over DIS is how the failure domain exploration is performed. Each exploration line in mLS contributes information on the derivative of each elementary failure domain, while DIS, along one direction, provides information on just the derivative of the union of all elementary failure domains.

Future extensions of the presented research could explore:

- Efficiency improvement by designing a modified Importance Sampling Density function.
- An extension to more general types of Gaussian excitation.
- The sensitivity calculation with respect to excitation parameters, i.e., frequencies of the Clough-Penzien model filters.

The above-mentioned issues are currently being investigated by the authors.

References

[1] Soong, T. and Grigoriu, M. (1993). Random Vibration of Mechanical and Structural Systems. Prentice Hall, Englewood Cliffs, New Jersey.

[2] Au, S., & Beck, J. (2001). First excursion probabilities for linear systems by very efficient importance sampling. Probabilistic Engineering Mechanics, 16 (3), 193–207.

[3] Katafygiotis, L., & Cheung, S. H. (2006). Domain decomposition method for calculating the failure probability of linear dynamic systems subjected to gaussian stochastic loads. Journal of Engineering Mechanics, 132 (5), 475–486.

[4] Misraji, M. A., Valdebenito, M. A., Jensen, H. A., & Mayorga, C. F. (2020). Application of directional importance sampling for estimation of first excursion probabilities of linear structural systems subject to stochastic Gaussian loading. Mechanical Systems and Signal Processing, 139, 106621.

[5] Valdebenito, M. A.,Wei, P., Song, J., Beer, M., & Broggi, M. (2021). Failure probability estimation of a class of series systems by multidomain line sampling. Reliability Engineering & System Safety, 213, 107673.

[6] Benfratello, S., Caddemi, S., & Muscolino, G. (2000). Gaussian and non-Gaussian stochastic sensitivity analysis of discrete structural system. Computers & Structures, 78 (1–3), 425–434.

[7] Jerez, D. J., Jensen, H. A., Valdebenito, M. A., Misraji, M. A., Mayorga, F., & Beer, M. (2022). On the use of Directional Importance Sampling for reliability-based design and optimum design sensitivity of linear stochastic structures. Probabilistic Engineering Mechanics, 70, 103368.

[8] Bjerager, P., & Krenk, S. (1989). Parametric sensitivity in first order reliability theory. Journal of Engineering Mechanics, 115 (7), 1577–1582.

[9] Wu, Y.-T. (1994). Computational methods for efficient structural reliability and reliability sensitivity analysis. AIAA Journal, 32 (8), 1717–1723.

[10] Papaioannou, I., Breitung, K., & Straub, D. (2013). Reliability sensitivity analysis with monte carlo methods. In Icossar 2013. University of N.Y.C.

[11] Jensen, H., Mayorga, F., & Valdebenito, M. (2015). Reliability sensitivity estimation of nonlinear structural systems under stochastic excitation: A simulation-based approach. Computer Methods in Applied Mechanics and Engineering, 289, 1–23.

[12] Au, S. (2005). Reliability-based design sensitivity by efficient simulation. Computers & Structures, 83 (14), 1048–1061.

[13] Valdebenito, M. A., Misraji, M. A., Jensen, H. A., & Franco Mayorga, C. (2021). Sensitivity estimation of first excursion probabilities of linear structures subject to stochastic gaussian loading. Computers & Structures, 248, 106482.

[14] Lu, Z., Song, S., Yue, Z., & Wang, J. (2008). Reliability sensitivity method by line sampling. Structural Safety, 30 (6), 517–532.

[15] Lee, I.-W., & Jung, G.-H. (1997). An efficient algebraic method for the computation of natural frequency and mode shape sensitivities—part i. distinct natural frequencies. Computers & Structures, 62 (3), 429–435.

[16] C. Schenk, G. Schuëller, Uncertainty Assessment of Large Finite Element Systems, Springer-Verlag, Berlin, Heidelberg, New York, 2005.

[17] G. Stefanou, The stochastic finite element method: Past, present and future, Computer Methods in Applied Mechanics and Engineering 198 (9-12) (2009) 1031–1051.

[18] Haftka, R. and Gürdal, Z. (1992). Elements of Structural Optimization. Kluwer, Dordrecht, The Netherlands, 3rd edition.

[19] Chopra, A. (1995). Dynamics of structures: theory and applications to earthquake engineering, Prentice Hall.

[20] Gautschi, W. (2012). Numerical analysis. In Birkhäuser Boston eBooks.

[21] Der Kiureghian, A. (2000). "The geometry of random vibrations and solutions by FORM and SORM." Probabilistic Engineering Mechanics, 15(1), 81–90.

[22] Koutsourelakis, P., Pradlwarter, H., and Schuëller, G. (2004). "Reliability of structures in high dimensions, part I: Algorithms and applications." Probabilistic Engineering Mechanics, 19(4), 409–417.

[23] Flanders, H. (1973). "Differentiation under the integral sign." The American Mathematical Monthly, 80(6), 615–627.

[24] Friswell, M. and Mottershead, J. (1995). Finite element model updating in structural dynamics. Kluwer Academic Publishers.

[25] Schuëller, G. I., & Pradlwarter, H. J. (2007). Benchmark study on reliability estimation in higher dimensions of structural systems – An overview. Structural Safety, 29(3), 167–182.

[26] Zerva, A. (2009). Spatial Variation of Seismic Ground Motions: Modeling and Engineering Applications (1st ed.). CRC Press.